

1 **PHOSPHORUS DYNAMICS NEAR BALD CYPRESS ROOTS IN A RESTORED WETLAND**

2 Colby J. Moorberg^{1*}, Michael J. Vepraskas², Christopher P. Niewhoener²

3
4 ¹Department of Agronomy
5 Kansas State University
6 2004 Throckmorton Plant Sciences Center
7 Manhattan, Kansas, 66506, USA
8 Office phone: 1-785-532-7207
9 Fax: 1-785-532-6094

10 Email: moorberg@ksu.edu

11 *Corresponding author

12
13 ²Department of Crop and Soil Sciences
14 North Carolina State University
15 Campus Box 7620
16 Raleigh, North Carolina 27695-7620, USA
17

18

19 **ACKNOWLEDGEMENTS**

20 The authors thank several people for their contributions to this research. Dr. Consuelo Arellano
21 assisted with the statistical analysis. Guillermo Ramirez assisted with porewater analyses. Justin
22 Milstein performed much of the minirhizotron root image processing. Dr. Mary Beth Kirkham
23 provided incites that improved the manuscript. Two anonymous reviewers provided useful
24 suggested revisions. The US Forest Service – Savannah River provided the minirhizotron camera
25 used in this study. Funding was provided by the United States Department of Agriculture
26 National Resources Inventory (USDA NRI), grant number 00415064; and the Water Resources
27 Research Institute of the University of North Carolina system (WRII), grant number 554982.
28 Contribution no. 18-148-J from the Kansas Agricultural Experiment Station.

29

30 This is the peer reviewed version of the following article: [Moorberg, C.J., Vepraskas, M.J. and
31 Niewhoener, C.P. (2017), Phosphorus Dynamics Near Bald Cypress Roots in a Restored
32 Wetland. *Soil Science Society of America Journal*, 81: 1652-1660.], which has been published in
33 final form at <https://doi.org/10.2136/sssaj2017.07.0228>. This article may be used for non-
34 commercial purposes in accordance with Wiley Terms and Conditions for Use of Self-Archived
35 Versions. This article may not be enhanced, enriched or otherwise transformed into a derivative
36 work, without express permission from Wiley or by statutory rights under applicable legislation.
37 Copyright notices must not be removed, obscured or modified. The article must be linked to
38 Wiley’s version of record on Wiley Online Library and any embedding, framing or otherwise
39 making available the article or pages thereof by third parties from platforms, services and
40 websites other than Wiley Online Library must be prohibited.

41 **ABSTRACT**

42 Phosphorus (P) dissolution occurs commonly in wetland soils restored from agricultural land.
43 Associated with the P release are high concentrations of dissolved organic carbon (DOC) and
44 Fe^{2+} . This field study evaluated the effect of a fluctuating water table on the root dynamics of
45 bald cypress (*Taxodium distichum* L. Rich.) to determine whether root death created soil
46 reduction microsites potentially contributing to P dissolution. The study site is a restored
47 Carolina bay wetland with organic soils. Root growth and death were monitored on 16, 6-year-
48 old bald cypress using minirhizotrons. Root dynamics, water table levels, and soil porewater
49 chemistry and redox potential in the root zone were monitored for two years. Soil solution
50 samples were analyzed for Fe^{2+} , pH, DOC, and P. High rates of root growth occurred during dry
51 conditions, while root death occurred during sustained periods of saturation, particularly within
52 20 cm of the surface. Cyclic changes in concentrations of Fe^{2+} , DOC, and dissolved total P
53 (DTP) were related to water table position, but not to changes in root numbers. Following
54 sustained periods of saturated conditions, redox potential decreased to 0 mV, Fe^{2+} increased to
55 $1.75 \text{ mg Fe}^{2+} \text{ L}^{-1}$, and DOC increased to 350 mg L^{-1} ; resulting in peak DTP concentrations of 750
56 $\mu\text{g L}^{-1}$, compared to $100 \mu\text{g L}^{-1}$ during dry periods. This study showed that in these high carbon
57 soils (approximately 20% organic C), rooting dynamics had minimal impact on changes in P
58 concentrations, and P dissolution was largely controlled by Fe-reduction processes occurring
59 within the C-rich soil matrix.

60

61 INTRODUCTION

62 Wetlands provide crucial ecosystem services such as wildlife habitat, groundwater
63 recharge, and surface water quality improvement (Galatowitsch and van der Valk, 1994). To
64 protect those services, federal and state regulations encourage wetland restoration to mitigate for
65 the loss of existing wetlands (Dahl and Allord, 1996). However, wetlands restored from
66 agricultural land have been observed to contribute phosphorus (P) to surface and drainage water,
67 thus further impairing water quality (e.g., Bruland et al., 2003; Aldous et al., 2007; Ardon et al.,
68 2010). In most of these restored wetlands, P dissolution was attributed to Fe reduction (Reddy
69 and DeLaune, 2008), though other mechanisms have been proposed (e.g. Jackson, 1964; Greaves
70 and Webley, 1965; Raghu and MacRae, 1966; Ponnampereuma, 1972; Turner and Gilliam, 1974a;
71 b; Stumm and Morgan, 1981; Borggaard et al., 2005). Soil reduction microsites (approximately
72 25 mm in diameter) form near areas of high concentrations of labile C, such as around dead roots
73 or in the rhizosphere where root exudates are high in concentration (Parkin, 1987). Because P
74 dissolution in reduced soils is associated closely to Fe reduction, it is likely that P dissolution can
75 occur at higher rates in these soil reduction microsites.

76 Bald cypress (*Taxodium distichum* L.Rich.) is a deciduous conifer commonly found in
77 the coastal southeastern U.S. in Carolina bays and other low-lying areas (Elias, 1980). The
78 species is known for extreme tolerance to flooding conditions due to its multiple metabolic and
79 physiological adaptations (Hook, 1984). Metabolic adaptations include anaerobic respiration and
80 increased alcohol dehydrogenase activity (Pezeshki et al., 1996) and the ability to accumulate
81 malate and shikimate in its roots (Li et al., 2010). Physiological adaptations include the
82 development of aerenchyma and pneumatophores, among others (Hook, 1984). Aerenchyma are
83 porous tissues in the stem and roots that allow diffusion of oxygen into the roots and rhizosphere,
84 and diffusion of sulfides, methane, and other toxic gases out to the atmosphere (Anderson and

85 Pezeshki, 2000; Colmer, 2003). Pneumatophores also allow CO₂, methane, and sulfide exchange
86 with the atmosphere (Brown, 1981; Purvaja et al., 2004; Mitsch and Gosselink, 2007).

87 Most studies examining root dynamics of bald cypress have focused on container or root-
88 box rhizotron methods to study the roots (Megonigal and Day, 1992; Pezeshki et al., 1996;
89 Moorberg et al., 2013, 2015; Slusher et al., 2014). These studies allowed environmental
90 conditions to be controlled during the experiment, such as water table depth or salinity. However
91 the studies use seedlings and saplings due to constraints on the size of the trees that can be
92 studied (Böhm, 1979a), and such trees may not have developed the adaptations needed to survive
93 anaerobic conditions.

94 Root systems of older trees can be studied *in-situ* using minirhizotron tubes, which are
95 clear tubes installed in the soil at an angle into the root system (Iversen et al. 2012). The use of
96 modified cameras allows for imaging of roots at a specified depth over time (Böhm, 1979b;
97 Iversen et al., 2012). Use of minirhizotron tubes has proven useful in wetland systems which
98 experience large fluctuations of root growth and death due to shallow water tables (Baker et al.,
99 2001; Iversen et al. 2012). Root dynamics of bald cypress have not previously been examined
100 using minirhizotron tubes *in-situ*. Further, the effects of tree root dynamics on the creation of soil
101 reduction microsites and the resulting dissolution of P has not been examined in the field in
102 conjunction with root-box rhizotrons.

103 Moorberg et al. (2015) used root-box rhizotron studies to examine the effects of the
104 rhizosphere of bald cypress on P dissolution, in mineral and organic soils, simulating flooded
105 conditions of restored Carolina bay wetlands. They observed P dissolution in both the matrix and
106 rhizosphere of bald cypress in both mineral and organic soils. They also observed significant root
107 death at depths greater than 42 cm and vigorous root growth near the surface within weeks

108 following saturation. This indicated that root “redistribution” was occurring in response to
109 changes in water table depths. Areas of vigorous root growth were associated with decreases in
110 dissolved P relative to matrix concentrations following three months of saturated conditions.

111 The goals of this study were to examine the effects of root dynamics of bald cypress *in-*
112 *situ* in a wetland restored from agricultural land, and to determine if increases in Fe^{2+} , dissolved
113 organic carbon (DOC), and dissolved P occurred following root death. The hypotheses tested
114 were: i) saturated and reduced conditions would result in root death in deep soil layers and
115 concurrent root growth near the soil surface, and ii) soil depths containing dead roots would
116 exhibit increased concentrations of DOC, Fe^{2+} , and increased P dissolution.

117 **METHODS**

118 *Site Description*

119 Juniper Bay (Figure 1) is a Carolina bay in Robeson County, NC, located approximately
120 10 km south of Lumberton (34°30'30"N 79°01'30"E). In 1999, the North Carolina Department
121 of Transportation (NCDOT) purchased this drained Carolina bay wetland to mitigate the
122 destruction of nearby wetlands caused by highway construction (Ewing, 2003). Juniper Bay is
123 oval-shaped, oriented lengthwise along a northwest-southeast transect, and is virtually flat with
124 an area of 256 ha. Organic soils (loamy, mixed, dysic, thermic Terric Haplosaprists) occupy
125 approximately 60% of Juniper Bay, largely in its center; mineral soils (sandy, siliceous, thermic
126 Aeric Alaquods) occupy the remainder. Soil properties are shown in Table 1. The wetland was
127 drained for agriculture beginning in 1971 (Figure 1), and was fertilized annually to meet soil-test
128 recommendations. It remained in crop production until 2001, at which time restoration activities
129 commenced (Ewing, 2003). Extensive background characterization of soils and monitoring of
130 hydrology in the bay was performed for five years prior to restoration. Preliminary restoration

131 efforts started in June 2003, and ditch filling began in late 2005. During and after restoration the
132 water quality has been monitored at the single, surface-water outflow structure on the southern
133 edge of the bay, and in groundwater samples throughout the site. Concentrations of P in the
134 surface water outflow have shown that P was lost from the bay following restoration of wetland
135 hydrology (Moorberg, 2014).

136 *Experimental Design*

137 The plot locations were determined by placing an equilateral triangle grid over the soils
138 map of the bay, and then selecting eight locations that were distributed across the organic and
139 mineral soil units (Figure 1). Four plots were in organic soils and four in mineral soil.

140 Bald cypress was chosen as the study species because it is one of the more common trees
141 planted at Juniper Bay during the restoration (N.C. Department of Environment, Health, and
142 Natural Resources (DEHNR), 2010), and has been previously studied in rhizotron and container
143 studies using Juniper Bay soils (Moorberg et al., 2013, 2015; Slusher et al., 2014). At each plot,
144 an initial tree survey was performed within 30 m of the existing groundwater monitoring wells to
145 identify bald cypress trees that were in good health and were 3 m in height or taller. Of the
146 eligible trees, two per plot were randomly selected for instrumentation.

147 *Minirhizotron Construction and Installation*

148 A minirhizotron system was installed for monitoring root growth and death throughout
149 the study (Figure 2). The minirhizotron tubes were 1.5 m long, acrylic 5.08 cm ID x 5.72 cm OD
150 (Piedmont Plastics, Morrisville, NC, USA). A hole was drilled at the top of each tube to engage
151 the locking mechanism of the minirhizotron camera indexing handle system. A 5.08 cm diameter
152 mechanical test plug (Oatey Supply Chain Services, Cleveland, Ohio, USA) coated with vacuum
153 grease was used to seal the bottom of the rhizotron tube. The tubes were installed at each

154 instrumented tree by boring an auger hole 60 cm from the base of the tree trunk with a 5.08 cm
155 diameter soil auger held at a 45° angle. A jig was used to hold the auger as close to 45° as
156 possible. Each rhizotron tube was then inserted into the auger hole. Exposed portions of each
157 tube were covered with adhesive aluminum flashing foil to limit light entering the tube, and to
158 offer some insulation. Each tube was secured with zip ties to wooden stakes.

159 *Root Analysis and Tree Measurements*

160 Roots were photographed monthly for a 2-year period on the days soil porewater was
161 collected. Images were obtained with a BTC-2 Camera System (Figure 2), BTC I-CAP software,
162 and the Indexing Handle System (Bartz Technology Corporation, Santa Barbara, CA, USA).
163 This system captures images of roots within “windows” 13.5 mm vertical by 18 mm horizontal
164 in size. Within the BTC I-CAP software, each root image is tagged with a minirhizotron tube
165 number, a session number, and a window number for future analysis.

166 Each image was analyzed for root length, diameter, color, growth, and death using
167 RootFly 2.0.2, a free, open-source software application designed for minirhizotron image
168 analysis. While RootFly does offer an automated image analysis algorithm for tracing new roots,
169 that feature was determined to have limited utility for this application. Thus, all roots were
170 identified and traced manually. The root data was summarized for depth intervals of 0-20 cm,
171 20-40 cm, and 40-60 cm for all tubes over all sessions. Root depth was determined using the
172 following equation:

$$D_r = W_n * 1.35 * \tan(\alpha) \quad \text{Eq. 1}$$

173 where D_r is the vertical root depth in cm, W_n is the window number, 1.35 is the window height in
174 cm, and α is the angle at which the minirhizotron tube is installed. In this study, a 45° angle was
175 used, which simplifies equation 1 to:

$$D_r = W_n * 1.35$$

Eq. 2

176 Summary data included total root number, total root length, and average width for each depth.

177 The diameter at breast height (DBH) and tree height were determined for each
178 instrumented tree on January 23, 2012, and again on June 17, 2013 using calipers, and measuring
179 tape and a clinometer, respectively.

180 *Soil Solution Sampling and Redox Measurements*

181 Soil solution was collected using Rhizon soil porewater samplers (standard 2.5 mm
182 rhizon sampler, 5 cm length, Rhizosphere Research Products, Wageningen, The Netherlands).
183 Before installation, Rhizon samplers were stored for 24 hours in deionized water with the
184 hydrophilic tips submerged to saturate them for use. The tubing of each sampler was extended
185 using approximately 40 cm of polytetrafluoroethylene (PTFE) tubing (0.8mm I.D.) to keep the
186 Luer lock of each sampler above the soil surface and/or ponded water. Rhizon sampler porous
187 tips are made of hydrophilic plastic (Shotbolt, 2009) which do not absorb P from solution as do
188 porous ceramic samplers (Zimmermann et al., 1978; Nagpal, 1982; Bottcher et al., 1984). As
189 described by Shotbolt (2009), the sampling tips have a mean pore size of 0.15 μm making
190 additional sample filtration unnecessary. Further, the Rhizon samplers do not change sample
191 redox conditions under normal sampling environments, and provide many other improvements
192 over porous cups for pore water sampling.

193 Platinum-tipped redox electrodes similar to that of Wafer et al. (2004) were used to
194 monitor redox potential. Measurements were made using a calomel reference electrode and a
195 voltmeter. Voltage readings were corrected relative to a standard hydrogen electrode by adding
196 250 mv to all field readings, as described by Vepraskas and Faulkner (2001). These readings
197 were not corrected for temperature. Again, based on redox corrections described by Vepraskas

198 and Faulkner, temperature differences in the range of 10 to 25°C would have resulted in
199 negligible differences in redox potentials of approximately 10 mV.

200 One soil solution sampler and three redox electrodes were installed at depths of 15 and 30
201 cm, at a distance of 30 cm from the edge of each tree trunk as depicted in Figure 2. A
202 polycarbonate plate (LEXAN, SABIC, Riyadh, Saudi Arabia) was first installed vertically in the
203 soil to hold the Rhizon samplers and redox electrodes at the desired depths. Each plate was
204 driven to the proper depth with a rubber mallet. Care was taken to limit root injury during the
205 installation of the plates, samplers, or electrodes. After the plate was inserted, an access hole was
206 excavated on one side of the plate to allow insertion of samplers and electrodes through holes
207 that were pre-drilled into the plate at the proper depths. The plates also allowed soil on one side
208 to remain undisturbed, while the access hole was refilled. After installation, the access hole was
209 backfilled with soil. The tubing and wires from the samplers and redox electrodes were secured
210 to a support constructed of polyvinyl chloride (PVC) pipe to ensure that wire and tube tips would
211 remain out of ponded water. Rhizon samplers were replaced every six months as recommended
212 by the manufacturer.

213 *Sampling and Analyses*

214 Soil pore-water sampling was performed monthly beginning in May 2011 and continued
215 for two years. Two amber-colored serum bottles (100 ml and 30 ml) were used to collect soil
216 pore water samples from each sampler. Prior to sampling, each 100 mL bottle was acid-washed
217 and dried, acidified with 0.250 ml of 12 M H₂SO₄, capped with a rubber septa and aluminum
218 cap, and evacuated to -78.5 kPa or greater pressure using an electric vacuum pump. The 100 ml
219 bottle was used for collecting samples for the analysis of dissolved Fe²⁺, dissolved reactive P

220 (DRP), and dissolved total P (DTP). The second bottle was left un-acidified and used to collect
221 samples to measure dissolved organic C (DOC) and pH.

222 Water samples were collected through a 25-gauge, 3.8 cm long, Luer-lock needle that
223 was attached to each Rhizon sampler. The sampling tube was first purged by inserting the needle
224 into an evacuated serum “purge” bottle to collect one Rhizon sampler volume (0.187 ml) (Soil
225 Moisture Equipment Corp., 2008) or more of water. After purging, the sampler needle was
226 inserted into the septa of the 30 ml serum bottle to collect approximately 15 ml of solution over
227 the course of four to six hours. Following this, the needle was inserted into the 100 ml bottle to
228 collect approximately 30 ml of solution overnight and collected first thing the next morning. The
229 unacidified samples were frozen upon the return from the field, and remained frozen until ready
230 for analysis. The acidified serum bottles were stored at room temperature in the dark until they
231 were analyzed for Fe^{2+} .

232 The concentration of Fe^{2+} in solution was determined using the phenanthroline method
233 (Joint Task Group: 20th Edition, 2005). The samples were reacted with the phenanthroline
234 reagent within 24 h of collection, and analyzed using a Shimadzu UV-2101PC
235 spectrophotometer (Shimadzu Scientific Instruments, Columbia, MD, USA) within 48 h of
236 sampling. A sample aliquot without phenanthroline reagent was used as a blank to correct the
237 absorbance reading for the impact of dissolved organic matter. Standard curves were produced
238 using ammonium iron (II) sulfate hexahydrate (99.997%). The remaining acidified samples were
239 then transferred to 20 mL scintillation vials for storage for future P determinations.

240 Subsamples for P determinations were submitted to the Environmental and Agricultural
241 Testing Service at NC State University. Dissolved reactive phosphorus was analyzed using a
242 multi-channel Quick Chem 8000 (Lachat Instruments, Milwaukee, WI, USA) using the method

243 described by Prokopy and Wendt (1994). Dissolved total P was analyzed using an Inductively
244 Coupled Plasma-Atomic Emission Spectrometer (Optima 2000, Perkin-Elmer, Waltham, MA,
245 USA).

246 The frozen samples were thawed and allowed to return to room temperature. Solution pH
247 was measured with a pH electrode. Because pH was not determined immediately in the field, soil
248 solution pH from the 30 cm depth samples were compared to samples from a concurrent study
249 that were collected from a well at the same depth that were analyzed for pH immediately. There
250 was no significant difference, therefore the authors conclude that freezing samples prior to
251 analyzing pH did not compromise sample pH. Following pH measurements, each sample was
252 immediately analyzed for DOC using a Shimadzu TOC-5050 total organic carbon analyzer
253 (Shimadzu Scientific Instruments, Columbia, MD, USA). Flocculation of DOC due to freezing
254 has been observed by Giesy and Briese (1978), but was not observed in this study. The standard
255 definition of dissolved organic carbon is organic C that passes through a 0.45 μm filter. Because
256 the Rhizon samplers used in this study have a smaller pore size (0.15 μm), in this paper we
257 operationally define DOC as dissolved organic C that passes through a 0.15 μm filter. The
258 smaller pore size in Rhizon samplers is inherent in the sampler design, but allows for porewater
259 collection under unsaturated conditions (Seeberg-Elverfeldt et al., 2005), a tradeoff the authors
260 deemed appropriate.

261 *Statistical Analysis*

262 The experimental design was a split-split plot design with the fixed effects including two
263 soil treatments (mineral and organic), two soil depths (15 cm and 30 cm) for soil solution
264 measurements, and the sampling date. Three depths were used for root data (0-20 cm, 20-40 cm,
265 and 40-60 cm). The two soil treatments were split among eight plots with four plots located on

266 each soil type. Each plot was replicated with two instrumented trees per plot location. The data
267 were analyzed in SAS 9.3 (SAS Institute Inc., 2011, Cary, NC, USA) using the PROC MIXED
268 procedure. Error bars shown in each figure depict the standard error of the mean. Multiple
269 comparisons were adjusted using the Tukey method in SAS. Natural log transformations were
270 used for DTP, DRP, DOP, and Fe^{2+} , and square root transformations were used for root counts
271 and root length sum data to conform to the normality assumptions of PROC MIXED in SAS.

272 **RESULTS**

273 *Rainfall and Water Table Depths*

274 The daily rainfall and the water table depths from the manual wells recorded at the time
275 of sampling are shown in Figure 3. Rainfall observed at Juniper Bay was below normal for both
276 2011 (956 mm) and 2012 (1020 mm) according to the USDA NRCS WETS table for Robeson
277 County (USDA-NRCS, 2013), which reports a normal rainfall range of 1085-1290 mm. As a
278 result, the average water table depth only went above the 15 cm depth (depth of the shallowest
279 soil porewater sampler) of the mineral soil once during the two-year study. Shallow water tables
280 did occur in the organic soils. This was likely due to the lower position of the organic soils on the
281 relatively flat Carolina bay landscape. Because one of the primary objectives of this study was to
282 observe changes in soil solution chemistry under saturated conditions in the field, the focus of
283 this paper going further will be on the organic soil results.

284 Saturated conditions occurred at the 30 cm depth from the beginning of the study in May
285 through June 2011, February 2012 through September 2012, and again from January through
286 May 2013. Saturated conditions occurred at the 15 cm depth for shorter durations than the 30 cm
287 depth. At 15 cm the organic soils were saturated at the first sampling in May 2011, then from

288 March 2012 through July 2012, then again from January 2013 through the end of the study in
289 May 2013.

290 *Redox Potential and pH*

291 The redox potentials at both the 15 and 30 cm depths over time are shown in Figure 4. On
292 average, redox potentials were significantly lower at 30 cm (158 mV, se ± 34 mV) than 15 cm
293 (378 mV, se ± 34 mV) ($p < 0.0001$) across all sampling events and both soil types. The lowest
294 redox potentials (approximately 0 mV for both depths) occurred during late spring and early
295 summer when the water table was within 30 cm of the surface and temperatures were increasing.
296 At a depth of 30 cm, redox potentials were low enough for reduced Fe^{2+} to occur, < 300 mV at
297 pH 4 (Vepraskas and Faulkner, 2001), from May to June 2011, and from January 2012 through
298 the conclusion of the study. At the 15 cm depth, Fe^{2+} would be expected in solution from May to
299 June 2011, March through November 2012, and from April through May 2013. The 15 cm depth
300 reached a maximum redox potential of approximately +700 mV during the fall months of 2011 –
301 the driest period of the study. The 30 cm depth reached +500 mV for the same period.

302 *Tree and Root Measurements*

303 The instrumented trees averaged 7.4 cm (se ± 0.2 cm,) DBH in January 2012, and
304 increased to 10.9 cm (se ± 0.2 cm) DBH by July of 2013. Tree heights were 5.5 m (se ± 0.4 m) in
305 January 2012, and increased to 5.7 m (se ± 0.4 m) by July 2013. Root counts from the
306 minirhizotron images are shown in Figure 5 for the 0-20, 20-40, and 40-60 cm depth intervals
307 over time with a square root-transformation. Root counts were highest at the surface and
308 decreased with depth for any specific time. The net changes over time are shown in Figure 6.
309 The largest increase in root growth occurred during the dry period in the summer months of
310 2011, followed by another smaller increase in root counts in the summer of 2012. Root death

311 occurred at all depths from August 2012 to May 2013, but was most pronounced in the upper 20
312 cm.

313 *Dissolved Organic Carbon*

314 Dissolved organic carbon (Figure 4) declined during the dry period of 2011 to minimums
315 of 150 mg DOC L⁻¹ in the 15 cm depth, and 250 mg DOC L⁻¹ in the 30 cm depth. Following a
316 rise in the water table and decreases in Eh at the two sampled depths in February 2012, DOC
317 rose to peaks of approximately 350 mg DOC L⁻¹ by June 2012. There was no significant
318 difference in DOC between depths.

319 *Ferrous Iron*

320 Reduced Fe concentrations (shown with a natural log-transformation in Figure 4) were
321 highest after sustained periods of saturated conditions and low redox potentials. Concentrations
322 in back-transformed values ranged from approximately 0 mg in the late summer of 2011 to 1.75
323 mg Fe²⁺ L⁻¹. In August and September 2012 the water table was between the 15 and 30 cm
324 depths creating oxidizing conditions in the 15 cm depth (Figure 3) and resulting in decreases in
325 Fe²⁺ at that depth (Figure 4). In the 30 cm depth, Fe²⁺ remained high with continued saturated
326 and reduced conditions. Concentrations declined slightly in November 2012 at both depths, then
327 increased again in May when water tables rose again.

328 *Phosphorus*

329 Dissolved total P concentrations (Figure 4) increased with increases in Fe²⁺ concentration
330 and decreases in redox potential. In addition, higher DTP concentrations (p=0.0008) were found
331 at the 30 cm depth than at the 15 cm depth across all sampling dates. This was likely due to the
332 30 cm depth having a lower redox potential (Figure 4). The highest DTP concentrations occurred
333 following sustained reduced conditions, particularly in May-July 2011, and again from August

334 2012 through February, 2013. Concentrations (in back-transformed values) of DTP ranged from
335 100 to 750 $\mu\text{g L}^{-1}$. Concentrations of DRP largely followed the same trends as DTP, but
336 differences were less pronounced (Supplemental Figure S1).

337 **DISCUSSION**

338 We hypothesized originally that dead roots would form microsites where Fe would be
339 reduced and DTP released. As a result, we expected to see concentrations of Fe^{2+} and DTP
340 increasing after roots had died. This was not observed, in part, because root growth and death
341 were not controlled by saturation and water table levels in the soil studied. Root numbers
342 increased from May 2011 through July 2012 at all depths, particularly in the top 20 cm, and
343 decreased thereafter through the conclusion of the study in May 2013. Drier than normal
344 conditions existed at Juniper Bay during this study, particularly during the late summer and fall
345 of 2011 when the water table dropped below 80 cm in the organic soils. Under dry conditions it
346 is common for trees to drop some leaves and reallocate resources to the production of new roots
347 (McDowell et al., 2008). However, root numbers continued to rise from February to May in
348 2012, even after the water table rose above a depth of 40 cm. Megonigal and Day (1992)
349 observed that bald cypress that experienced alternating flooded and dry soil conditions exhibited
350 increased root production relative to continuously flooded sites, because intermittent flooding
351 allowed the trees adequate moisture during times when the soil was not waterlogged.

352 Changes in root numbers were not related to redox potential. Increases in root numbers
353 from May 2011 through July 2012 occurred during a period when the redox potential increased
354 from approximately 0 to 700 mv (15 cm depth) and declined back to approximately 0 mv. This
355 indicated the root increases in the upper 20 cm occurred during periods of aerobic as well as
356 anaerobic, Fe-reduced conditions. The bald cypress roots of the trees studied were adapted to

357 grow under anaerobic conditions. Further, had this study been conducted during a wetter period,
358 similar results in root growth would be expected, due to root numbers having no relation to redox
359 potential.

360 In root-box rhizotron studies, several researchers have observed root growth in the soil
361 surface concurrent with root death in deeper, more reduced soil layers (Schat, 1984; Moorberg et
362 al., 2013, 2015; Slusher et al., 2014). However, that pattern of root redistribution was not
363 observed in this minirhizotron-tube study. This could be due to the age and pre-conditioning of
364 the trees studied, which allowed the roots to develop adaptations (e.g., aerenchyma) that
365 conditioned them to survive in anaerobic environments. In root-box rhizotron studies and other
366 container studies, tree size are limited to seedlings and saplings which may be experiencing
367 saturated soil conditions for the first time, and must develop adaptations or shift root distribution
368 to adjust to anaerobic conditions. The 6-year-old trees at Juniper Bay had already experienced
369 six seasonal water table fluctuations, while the saplings used in previous root-box rhizotron
370 studies (Schat, 1984; Moorberg et al., 2013, 2015; Slusher et al., 2014) were experiencing
371 saturation for the first time. Thus, pre-conditioning tree saplings prior to use in container studies
372 simulating wetland hydrology may improve the relevancy of such experiments to field
373 conditions.

374 DOC fluctuations were not clearly related to root growth. We expected to see DOC
375 concentrations increase following periods of root death but this was not observed. The largest
376 increases in DOC occurred from January through September 2012 when root numbers at all
377 depths were either increasing or remaining constant. The source for the DOC may have been
378 decomposing organic tissues in the matrix of these organic soil materials.

379 Concentrations of Fe^{2+} were related to water table levels, and reached peak values
380 approximately 1 to 2 months after each depth was saturated. Once that depth became oxidized
381 following a drop in the water table, concentrations of Fe^{2+} immediately declined. Peak
382 concentrations in Fe^{2+} occurred when the soil was below a redox potential of 300 mV (Figure 4),
383 the redox potential at which Fe would be expected to be reduced for a soil pH of 4, according to
384 the assumptions listed by Vepraskas and Faulkner (2001).

385 Concentrations of Fe^{2+} varied in a pattern similar to changes in DOC with the highest
386 concentrations for both occurring within the May to September period in 2011 and 2012. This
387 pattern showed no apparent relationship to changes in root growth, again indicating that root
388 death was not supplying organic C used by microbes that utilized Fe^{3+} compounds as electron
389 acceptors. The organic C that was oxidized when Fe was being reduced apparently came for the
390 matrix of the organic soils.

391 Also during the 2012 drawdown, DTP concentrations dropped from peak concentrations
392 ($600\text{-}700\ \mu\text{g L}^{-1}$) reached following three to four months of prolonged saturated, reduced
393 conditions at the 15 cm depth, while DTP concentrations remained high in the still saturated and
394 reduced 30 cm depth. Because the DOC concentration did not depict any sudden changes during
395 this period, precipitation of Fe^{3+} is the likely cause of the decreases in DTP concentration, thus
396 indicating the reduction and oxidation of Fe is controlling P concentrations in this system.
397 Increases in DTP concentrations at both depths occurred following soil saturation, with peak
398 concentrations occurring 3 to 4 months after the onset of saturation, which were within the time
399 frame noted for peaks in Fe^{2+} . Patterns in DRP concentrations through time mirrored those of
400 DTP, though at lower concentrations (Supplemental Figure 1).

401 These results for Fe, DOC, and DTP matched those of Moorberg et al. (2013, 2015), who
402 found that P dissolution, as well as the precipitation of dissolved P, was controlled primarily by
403 Fe reduction and oxidation. The presence of living and/or dead roots did not cause additional
404 dissolution of P above concentrations found in the matrix for the soil material having an organic
405 C of 19.5% (based on C measurements by Abit, (2009). Further, P concentrations under
406 sustained saturated and reduced conditions could be limited by the presence of living roots that
407 contain aerenchyma. From those results, it can be inferred that the dissolution of P in this field
408 study is the product of reduction processes occurring in the matrix, and that labile C was not
409 limiting to soil reduction in the Histosol studied. Concentrations of DOC in this study exhibited
410 minimal changes through the dry and wet seasons, while both DTP and Fe²⁺ showed large
411 variations in concentrations with changes through the seasons. Further, P concentrations
412 increased with increases in Fe²⁺ as the soil became more reduced. Upon the water table dropping
413 below the 15 cm depth in August of 2012, and the resulting oxidizing conditions, Fe began to
414 precipitate, and DTP concentrations immediately declined. Therefore, P dissolution is likely Fe-
415 controlled in this restored, Carolina bay Histosol.

416 In addition, despite this study being conducted during an abnormally dry period, we
417 expect the results to be representative of what might occur under normal rainfall due to the
418 correspondence of these observations to those of Moorberg et al. (2013, 2015), which were
419 conducted in controlled, saturated conditions in a greenhouse setting.

420 **CONCLUSIONS**

421 The goals of this study were to examine the growth and death of bald cypress roots *in-situ*
422 in a wetland restored from agricultural land, and to determine concentrations of Fe²⁺, DOC, and
423 DTP increased after roots died. Root growth and death had no apparent effect on concentrations

424 of Fe²⁺, DOC, or DTP. This indicated that while dead roots might be microsites for Fe reduction
425 in some soils, they had little effect in reducing processes here. This is most likely because the
426 soil matrix of the organic soil studied contained adequate labile C in its matrix to enable Fe
427 reducing reactions. Dissolution of P did occur during extended periods of saturation, and was
428 likely controlled by Fe reduction. Previous and concurrent root-box rhizotron studies showed
429 that contributions of labile C from the rhizospheres of bald cypress growing in soils with high
430 organic matter content, such as the soils used in this study, did not cause additional soil P
431 dissolution, and that is assumed to be the case for this field study as well. However, the
432 contribution of root dynamics on P dissolution in soils with low amounts of organic matter and
433 labile C is still unknown and needs further research.

434 **REFERENCES**

- 435 Abit, S. 2009. Hydrologic effects on subsurface fates and transport of contaminants. Ph.D. diss.
436 North Carolina State Univ. Raleigh.
- 437 Aldous, A., C. Craft, C. Stevens, M. Barry, and L. Bach. 2007. Soil phosphorus release from a
438 restoration wetland. *Wetlands* 27: 1025–1035.
- 439 Anderson, P.H., and S.R. Pezeshki. 2000. The effects of intermittent flooding on seedlings of
440 three forest species. *Photosynthetica* 37(4): 543–552.
- 441 Ardon, M., J.L. Morse, M.W. Doyle, and E.S. Bernhardt. 2010. The water quality consequences
442 of restoring wetland hydrology to a large agricultural watershed in the Southeastern
443 Coastal Plain. *Ecosystems* 13: 1060–1078.
- 444 Baker, T.T., W.H. Conner, B.G. Lockaby, J.A. Stanturf, and M.K. Burke. 2001. Fine root
445 productivity and dynamics on a forested floodplain in South Carolina. *Soil Sci. Soc. Am.*
446 *J.* 65(2): 545–556.
- 447 Böhm, W. 1979a. Container methods. p. 95–114. *In* Billings, W.D., Golley, F., Lange, O.L.,
448 Olson, J.S. (eds.), *Methods of studying root systems*. Ecological Studies. Springer-
449 Verlag, Berlin.
- 450 Böhm, W. 1979b. Glass wall methods. p. 61–70. *In* Billings, W.D., Golley, F., Lange, O.L.,
451 Olson, J.S. (eds.), *Methods of studying root systems*. Ecological Studies. Springer-
452 Verlag, Berlin.
- 453 Borggaard, O.K., B. Raben-Lange, A.L. Gimsing, and B.W. Strobel. 2005. Influence of humic
454 substances on phosphate adsorption by aluminum and iron oxides. *Geoderma* 127(3–4):
455 270–279.
- 456 Bottcher, A.B., L.W. Miller, and R.L. Campell. 1984. Phosphorus adsorption in various soil-
457 water extraction cup materials: effect of acid wash. *Soil Sci.* 13: 239–244.
- 458 Brown, S. 1981. A comparison of the structure, primary productivity, and transpiration of
459 cypress ecosystems in Florida. *Ecol. Monogr.* 51(4): 403–427.
- 460 Bruland, G.L., M.F. Hanchey, and C.J. Richardson. 2003. Effects of agriculture and wetland
461 restoration on hydrology, soils, and water quality of a Carolina bay complex. *Wetl. Ecol.*
462 *Manag.* 11(3): 141–156.
- 463 Colmer, T.D. 2003. Long-distance transport of gases in plants: a perspective on internal aeration
464 and radial oxygen loss from roots. *Plant Cell Environ.* 26(1): 17–36.
- 465 Dahl, T.E., and G.J. Allord. 1996. History of wetlands in the conterminous United States. *In*
466 Fretwell, J.D., Williams, J.S., Redman, P.J. (eds.), *National Water Summary on Wetland*
467 *Resources*. USGS Water-Supply Paper 2425: 19–26.

- 468 Elias, T.S. 1980. The complete trees of North America: field guide and natural history. Outdoor
469 Life/Nature Books, New York.
- 470 Ewing, J.M. 2003. Characterization of soils in a drained Carolina bay wetland prior to
471 restoration. Ph.D. diss. North Carolina State Univ., Raleigh.
- 472 Galatowitsch, S.M., and A. van der Valk. 1994. Restoring prairie wetlands: an ecological
473 approach. Iowa State University Press, 1998, Ames.
- 474 Giesy, J.P., and L.A. Briese. 1978. Particulate formation due to freezing humic waters. Water
475 Resour. Res. 14(3): 542–544.
- 476 Greaves, M.P., and D.M. Webley. 1965. A study of the breakdown of organic phosphates by
477 micro-organisms from the root region of certain pasture grasses. J. Appl. Bacteriol. 28:
478 454–465.
- 479 Hook, D. 1984. Waterlogging tolerance of lowland tree species of the South. J. Appl. For. 8(3):
480 136–149.
- 481 Iversen, C.M., M.T. Murphy, M.F. Allen, J. Childs, D.M. Eissenstat, E.A. Lilleskov, T.M.
482 Sarjala, V.L. Sloan, and P.F. Sullivan. 2012. Advancing the use of minirhizotrons in
483 wetlands. Plant Soil 352(1–2): 23–39.
- 484 Jackson, M.L. 1964. Chemistry of the soil. p. 71–141. In Bear, F.E. (ed.), Van Nostrand-
485 Reinhold, Princeton, New Jersey.
- 486 Joint Task Group: 20th Edition. 2005. Iron. p. 3–76. In Standard Methods Committee, 1997
487 (ed.), Standard methods for the examination of water and wastewater. American Public
488 Health Association, Washington, DC, USA.
- 489 Li, C., Z. Zhong, Y. Geng, and R. Schneider. 2010. Comparative studies on physiological and
490 biochemical adaptation of *Taxodium distichum* and *Taxodium ascendens* seedlings to
491 different soil water regimes. Plant Soil 329(1–2): 481–494.
- 492 McDowell, N., W.T. Pockman, C.D. Allen, D.D. Breshears, N. Cobb, T. Kolb, J. Plaut, J.
493 Sperry, A. West, D.G. Williams, and E.A. Yezzer. 2008. Mechanisms of plant survival
494 and mortality during drought: why do some plants survive while others succumb to
495 drought? New Phytol. 178(4): 719–739.
- 496 Megonigal, J.P., and F.P. Day. 1992. Effects of flooding on root and shoot production of bald
497 cypress in large experimental enclosures. Ecology 73(4): 1182–1193.
- 498 Mitsch, W.J., and J.G. Gosselink. 2007. Wetlands. Wiley, Hoboken, N.J.
- 499 Moorberg, C.J. 2014. Phosphorus fluxes in a restored Carolina Bay wetland following eight
500 years of restoration. p. 134–183. In Dynamics of P Release from Wetlands Restored on
501 Agricultural Land. Ph.D. diss. North Carolina State Univ., Raleigh.

- 502 Moorberg, C.J., M.J. Vepraskas, and C.P. Niewoehner. 2013. Dynamics of P dissolution
503 processes in the matrix and rhizospheres of bald cypress growing in saturated soil.
504 *Geoderma* 202–203: 153–160.
- 505 Moorberg, C.J., M.J. Vepraskas, and C.P. Niewoehner. 2015. Phosphorus Dissolution in the
506 Rhizosphere of Bald Cypress Trees in Restored Wetland Soils. *Soil Sci. Soc. Am. J.*
507 79(1): 343.
- 508 Nagpal, N.K. 1982. Comparison among and evaluation of ceramic porous cup soil water
509 samplers for nutrient transport studies. *Can. J. Soil Sci.* 62(4): 685–694.
- 510 N.C. Department of Environment, Health, and Natural Resources (DEHNR). 2010. Juniper Bay
511 wetland mitigation site 2010 annual monitoring report. Raleigh.
- 512 Parkin, T.B. 1987. Soil microsites as a source of denitrification variability. *Soil Sci. Soc. Am. J.*
513 51(5): 1194.
- 514 Pezeshki, S.R., J.H. Pardue, and R.D. DeLaune. 1996. Leaf gas exchange and growth of flood-
515 tolerant and flood-sensitive tree species under low soil redox conditions. *Tree Physiol.*
516 16(4): 453–458.
- 517 Ponnampereuma, F.N. 1972. The chemistry of submerged soils. *Adv. Agron.* 24: 29–96.
- 518 Prokopy, W.R., and K. Wendt. 1994. QuikChem Method 10-115-01-1-B: Orthophosphate in
519 waters. Lachat Instruments, Loveland.
- 520 Purvaja, R., R. Ramesh, and P. Frenzel. 2004. Plant-mediated methane emission from an Indian
521 mangrove. *Glob. Change Biol.* 10(11): 1825–1834.
- 522 Raghu, K., and I.C. MacRae. 1966. Occurrence of phosphate-dissolving micro-organisms in the
523 rhizosphere of rice plants and in submerged soils. *J. Appl. Bacteriol.* 29(3): 582–586.
- 524 Reddy, R., and R.D. DeLaune. 2008. Biogeochemistry of wetlands: science and applications.
525 CRC Press Taylor and Francis Group, New York.
- 526 Schat, H. 1984. A comparative ecophysiological study on the effects of waterlogging and
527 submergence on dune slack plants: growth, survival and mineral nutrition in sand culture
528 experiments. *Oecologia* 62: 279–286.
- 529 Seeberg-Elverfeldt, J., M. Schlüter, T. Feseker, and M. Kölling. 2005. Rhizon sampling of
530 porewaters near the sediment-water interface of aquatic systems. *Limnol. Oceanogr.*
531 *Methods* 3: 361–371.
- 532 Shotbolt, L. 2009. Pore water sampling from lake and estuary sediments using Rhizon samplers.
533 *J. Paleolimnol.* 44(2):695–700.
- 534 Slusher, C.E., M.J. Vepraskas, and S.W. Broome. 2014. Evaluating responses of four wetland
535 plant species to different hydroperiods. *J. Environ. Qual.* 43(2): 723–731.

- 536 Soil Moisture Equipment Corp. 2008. 1908D2.5L10 Micro sampler operating instructions. Santa
537 Barbara.
- 538 Stumm, W., and J.J. Morgan. 1981. Aquatic chemistry: an introduction emphasizing chemical
539 equilibria in natural waters. Wiley, New York.
- 540 Turner, F.T., and J.W. Gilliam. 1974a. Effect of moisture and oxidation status of alkaline rice
541 soils on the adsorption of soil phosphorus by an anion resin. *Plant Soil* 45(2): 353–363.
- 542 Turner, F.T., and J.W. Gilliam. 1974b. Increased P diffusion as an explanation of increased P
543 availability in flooded rice soils. *Plant Soil* 45(2): 365–377.
- 544 USDA-NRCS. 2013. Robeson County, NC WETS Table. *Clim. Anal. Wetl. Cty.* Available at
545 <http://www.wcc.nrcs.usda.gov/ftpref/support/climate/wetlands/nc/37155.txt> (verified 26
546 October 2013).
- 547 Vepraskas, M.J., and S.P. Faulkner. 2001. Redox chemistry of hydric Soils. p. 85–105. *In*
548 Richardson, J.L., Vepraskas, M.J. (eds.), *Wetland soils: genesis, hydrology, landscapes,*
549 *and classification.* CRC Press, Boca Raton, FL.
- 550 Wafer, C.C., J.B. Richards, and D.L. Osmond. 2004. Construction of platinum-tipped redox
551 probes for determining soil redox potential. *J. Environ. Qual.* 33(6): 2375–2379.
- 552 Zimmermann, C.F., M.T. Price, and J.R. Montgomery. 1978. A comparison of ceramic and
553 Teflon in situ samplers for nutrient pore water determinations. *Estuar. Coast. Mar. Sci.*
554 7(1): 93–97.
- 555
- 556

557 **TABLES**558 **Table 1. Summary of soil chemical and physical properties for the mineral and organic**
559 **soils from Juniper Bay.†**

Soil Properties	Unit	Mineral Soil	Organic Soil
Organic C	% w/w	3.5	19.5
‡Total P	mg cm ⁻³	0.21	0.13
Mehlich III P	mg cm ⁻³	0.08	0.12
pH		4.9	4.2
Surface Texture		Loamy Sand	Sapric material
Bulk Density	g cm ⁻³	1.45	0.62
§Porosity		0.48	0.63
§Saturated Conductivity	m d ⁻¹	3.00	1.17

560 †Table originally published in Moorberg et al. (2015) and provided here
561 with permission.562 ‡Values from Moorberg et al. (2014 chap. Phosphorus Fluxes in a
563 Restored Carolina Bay Wetland Following Eight Years of Restoration)

564 §Values from Abit (2009)

565 **LIST OF FIGURES**

566 **Figure 1. Map of Juniper Bay and Study Sites. Eight study sites were split between the two**
567 **soil types, mineral and organic, at Juniper Bay. Two trees were instrumented at each of the**
568 **eight study sites, with four sites located on mineral soils, and four on organic soils.**

569 **Figure 2. Minirhizotron tube, soil sampler, and groundwater well instrumentation. As**
570 **shown in picture A, each studied tree was instrumented with a (left to right) groundwater**
571 **monitoring [manual] well, a rhizon soil porewater sampler and redox electrode station, and**
572 **a minirhizotron tube.**

573 **Figure 3. Average water table depths for the mineral and organic soils and daily rainfall**
574 **data for Juniper Bay. The error bars depict standard error. Water table depths are shown**
575 **for the duration of the field study. The solid black line at depth 0 depicts the soil surface,**
576 **while the long-dashed line and the short-dashed line depict the location of the 15 cm and 30**
577 **cm depth samplers, respectively.**

578 **Figure 4. Redox potential (A), concentration of DOC (B), concentration (natural log-**
579 **transformed) of Fe^{2+} (C), and concentration of (natural log-transformed) DTP (D) at 15**
580 **and 30 cm in depth over time for the organic soil. The error bars in each panel depict**
581 **standard error.**

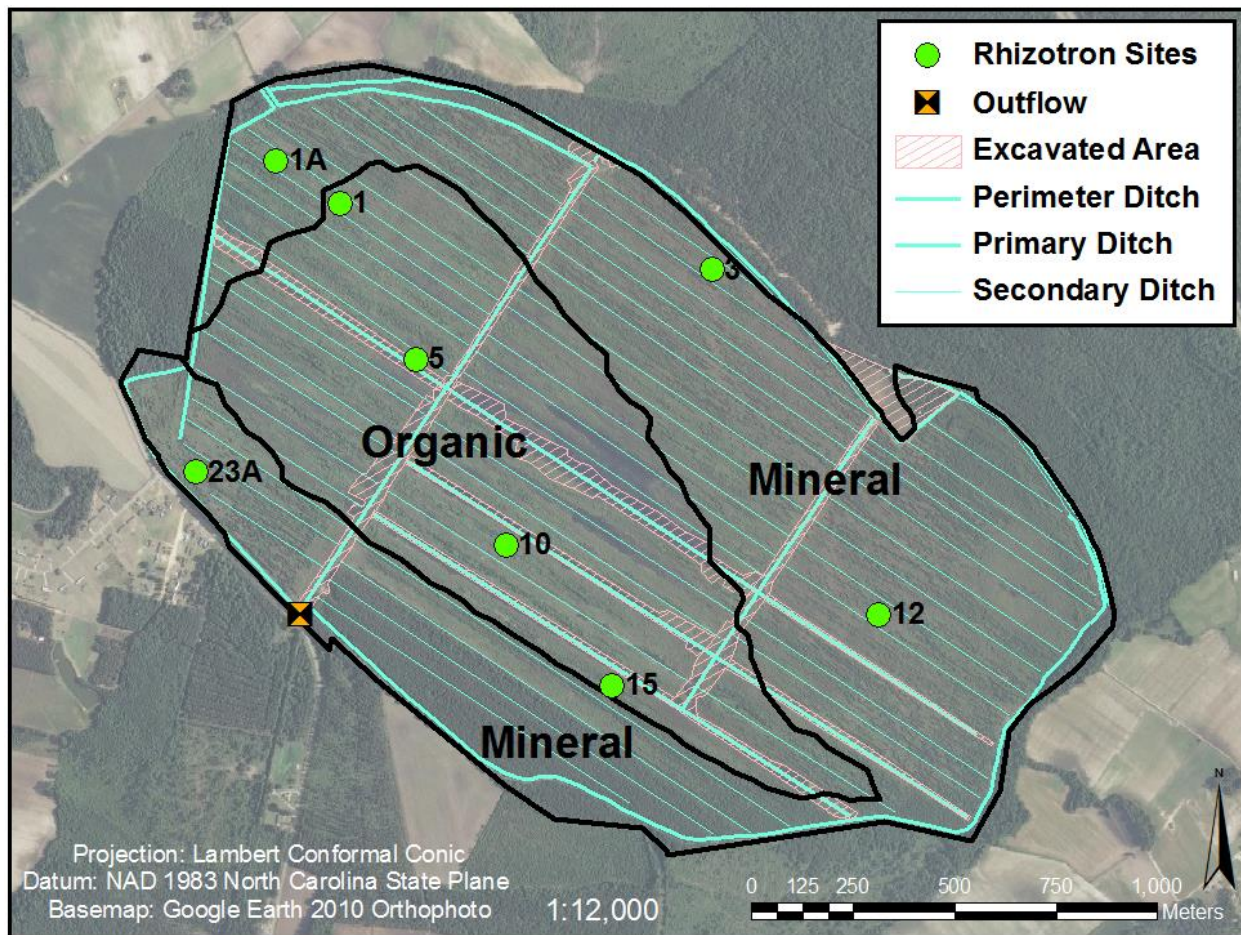
582 **Figure 5. Root counts (square root-transformed) from minirhizotron images for 0-20, 20-**
583 **40, and 40-60 cm depths of the organic soil. The y-axis is the square root of the number of**
584 **roots observed for each of the three depths for a given sampling event. Open symbols**
585 **indicate that the water table is deeper than the depth interval. Error bars depict the**
586 **standard error.**

587 **Figure 6. Change in root count by depth over time of the organic soil. The values on the y-**
588 **axes depict the change in overall root count for each depth from the count of the previous**
589 **month. Positive numbers depict new root growth, while negative values show root death.**
590 **The scale of the y-axis is different for each depth. The error bars depict standard error.**

591 **LIST OF SUPPLEMENTAL FIGURES**

592 **Supplemental Figure 1. Concentration (natural log-transformed) of DRP by depth over**
593 **time. The y-axis shows natural log-transformed concentrations of DRP concentration, with**
594 **time on the x-axis. The concentration of DRP increased slightly during periods of high Fe²⁺**
595 **concentrations. The error bars depict standard error. The observed concentrations ranged**
596 **in back-transformed values of approximately 75 µg L⁻¹ to 500 µg L⁻¹.**

597



598

599 **Figure 1. Map of Juniper Bay and Study Sites. Eight study sites were split between the two**
 600 **soil types, mineral and organic, at Juniper Bay. Two trees were instrumented at each of the**
 601 **eight study sites, with four sites located on mineral soils, and four on organic soils.**

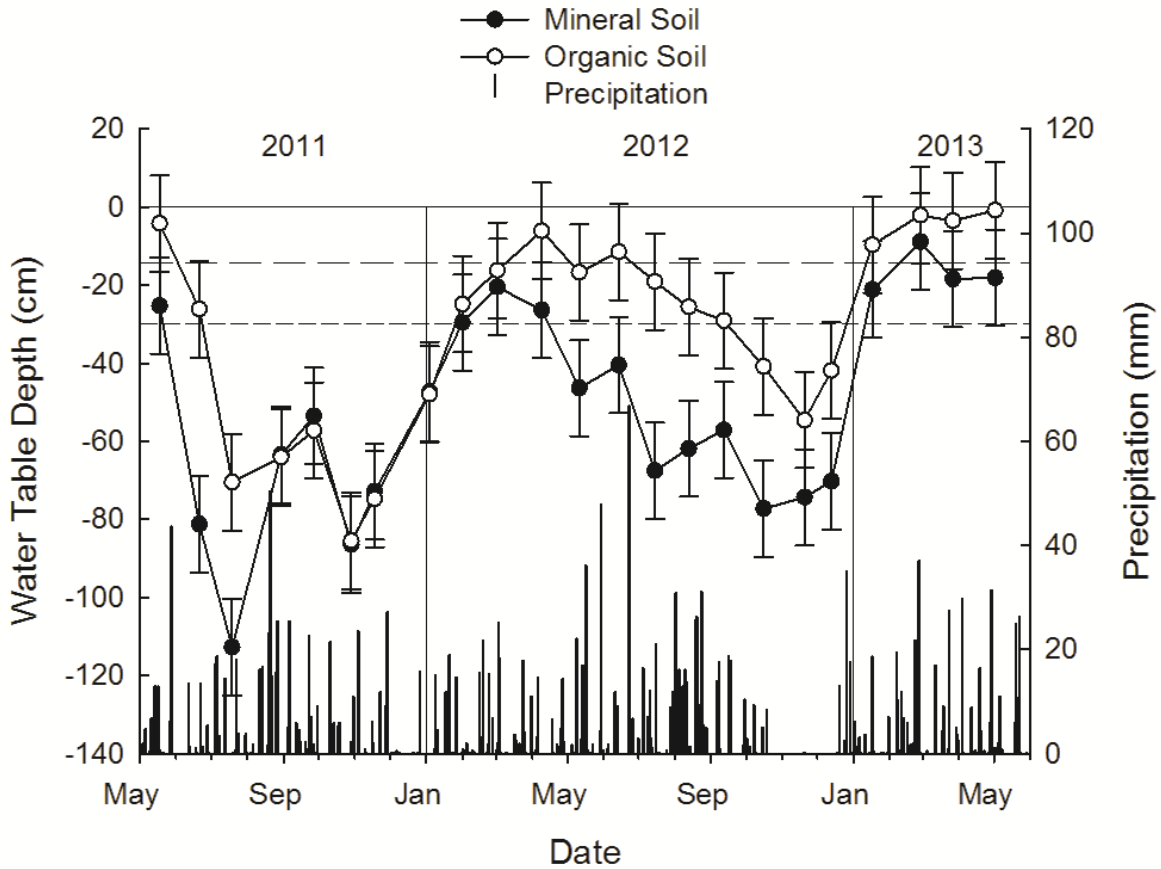
602



603

604 **Figure 2. Minirhizotron tube, soil sampler, and groundwater well instrumentation. As**
605 **shown in picture A, each studied tree was instrumented with a (left to right) groundwater**
606 **monitoring [manual] well, a rhizon soil porewater sampler and redox electrode station, and**
607 **a minirhizotron tube.**

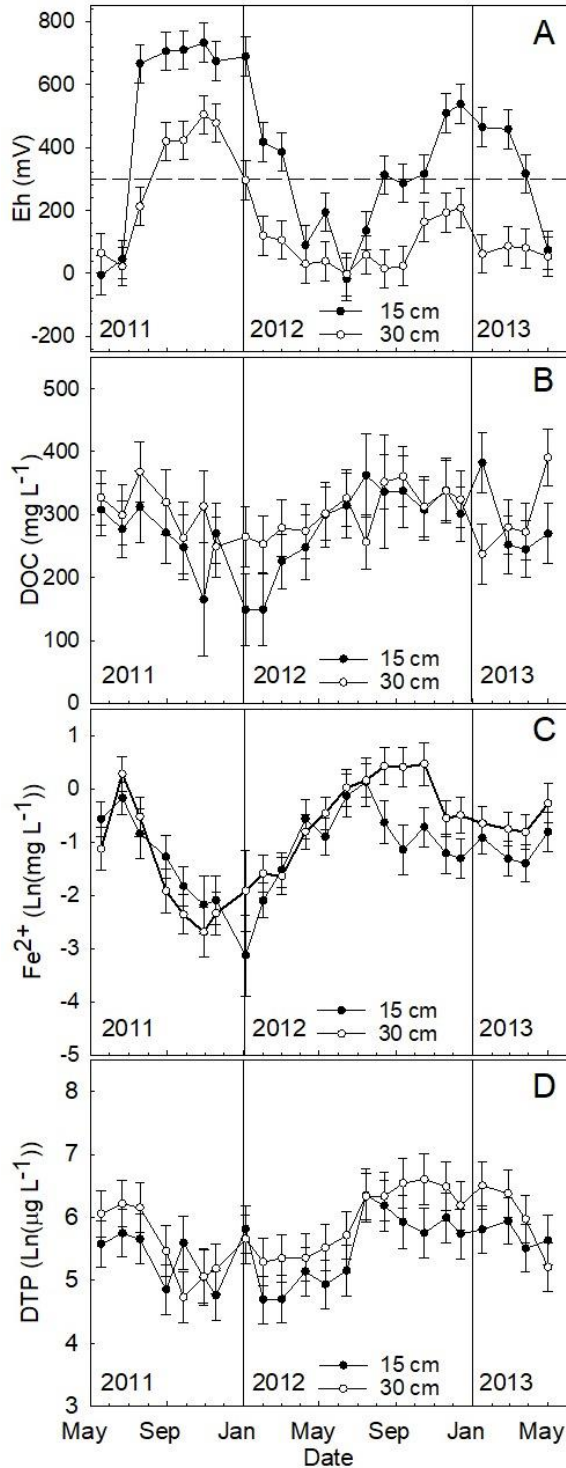
608



609

610 **Figure 3. Average water table depths for the mineral and organic soils and daily rainfall**
 611 **data for Juniper Bay. The error bars depict standard error. Water table depths are shown**
 612 **for the duration of the field study. The solid black line at depth 0 depicts the soil surface,**
 613 **while the long-dashed line and the short-dashed line depict the location of the 15 cm and 30**
 614 **cm depth samplers, respectively.**

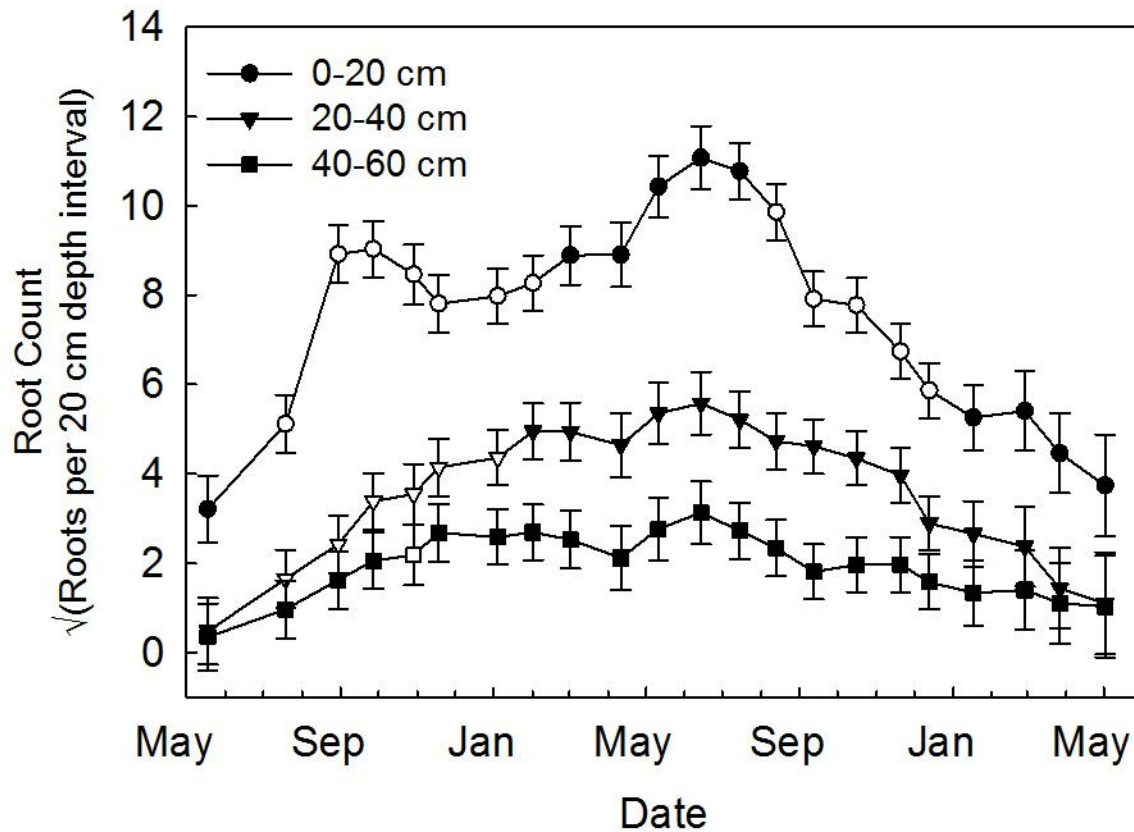
615



616

617 **Figure 4. Redox potential (A), concentration of DOC (B), concentration (natural log-**
 618 **transformed) of Fe²⁺ (C), and concentration of (natural log-transformed) DTP (D) at 15**
 619 **and 30 cm in depth over time for the organic soil. The error bars in each panel depict**
 620 **standard error.**

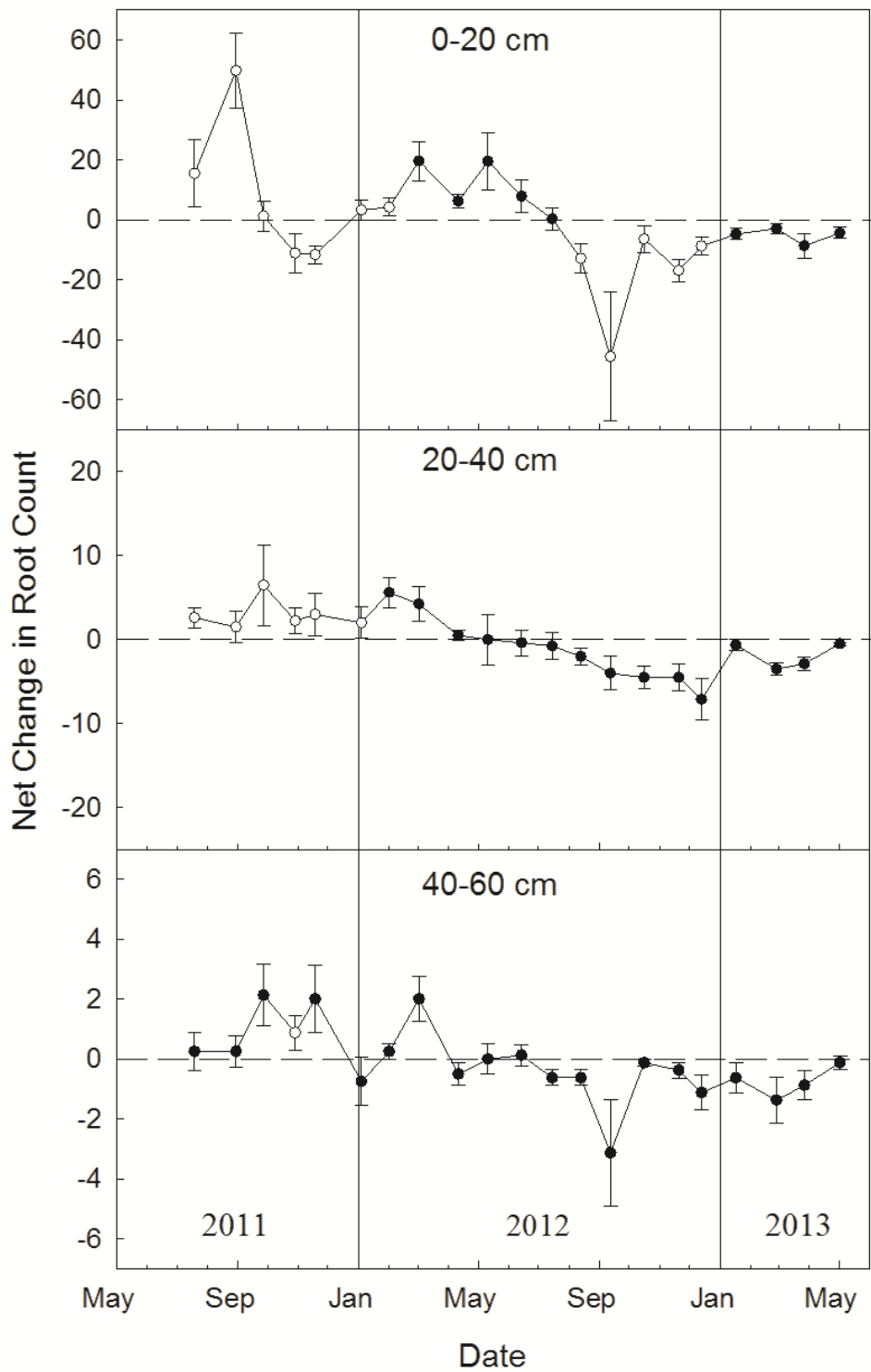
621



622

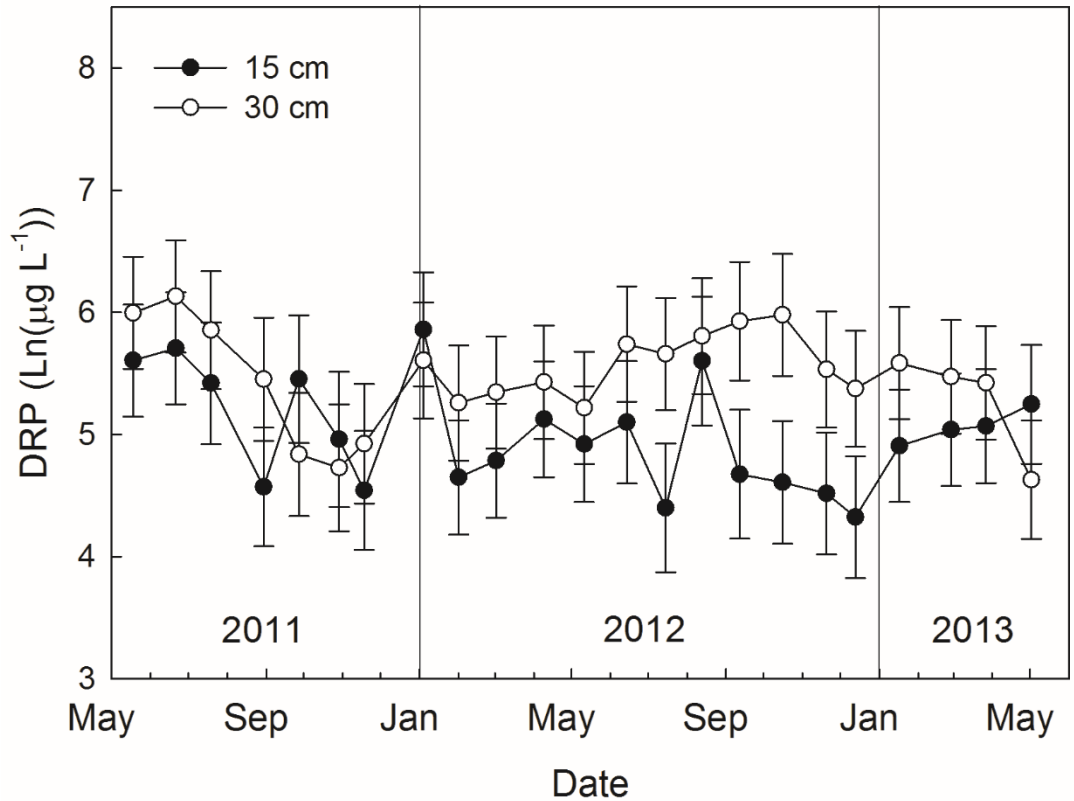
623 **Figure 5. Root counts (square root-transformed) from minirhizotron images for 0-20, 20-**
 624 **40, and 40-60 cm depths of the organic soil. The y-axis is the square root of the number of**
 625 **roots observed for each of the three depths for a given sampling event. Open symbols**
 626 **indicate that the water table is deeper than the depth interval. Error bars depict the**
 627 **standard error.**

628



629

630 **Figure 6. Change in root count by depth over time of the organic soil. The values on the y-**
 631 **axes depict the change in overall root count for each depth from the count of the previous**
 632 **month. Positive numbers depict new root growth, while negative values show root death.**
 633 **The scale of the y-axis is different for each depth. The error bars depict standard error.**



634

635 **Supplemental Figure 1. Concentration (natural log-transformed) of DRP by depth over**
 636 **time. The y-axis shows natural log-transformed concentrations of DRP concentration, with**
 637 **time on the x-axis. The concentration of DRP increased slightly during periods of high Fe²⁺**
 638 **concentrations. The error bars depict standard error. The observed concentrations ranged**
 639 **in back-transformed values of approximately 75 µg L⁻¹ to 500 µg L⁻¹.**

640